INTERNATIONAL CENTRE FOR NUMERICAL METHODS IN ENGINEERING

A CONSORTIUM OF Generalitat de Catalunya, UNIVERSITAT POLITÈCNICA DE CATALUNYA BARCELONATECH

IN COOPERATION WITH unesco, CERCA Centres de Recerca de Catalunya

SPHERIC June 2025 - Barcelona

Stabilised SPH formulations in large strain solid mechanics

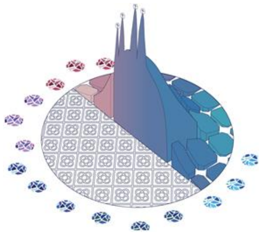

Javier Bonet, CIMNE

A.J. Gil, (Swansea University) &

C.H. Lee (Glasgow University)

A. Ghavamian, J. Haider, C.J. Runcie, P. Refachinho,

T. Jaugielavicius

OUTLINE

- Motivation & Aims
- Solid dynamics as 1st order conservation laws
  - Large deformations – mappings
  - Dynamic conservation laws
  - Jump conditions
  - Linear elasticity
  - ALE & URL formulations
- Stable Smooth Particle Hydrodynamics
  - SPH Discretization
  - Ballistic Energy and stability
- Dynamic crack propagation
  - Mode I transonic and intersonic analytical solutions
  - Mode II transonic analytical solutions
  - SPH Implementations
- Examples
- Summary and Conclusions

2

CIMNE

Motivation – Previous Work

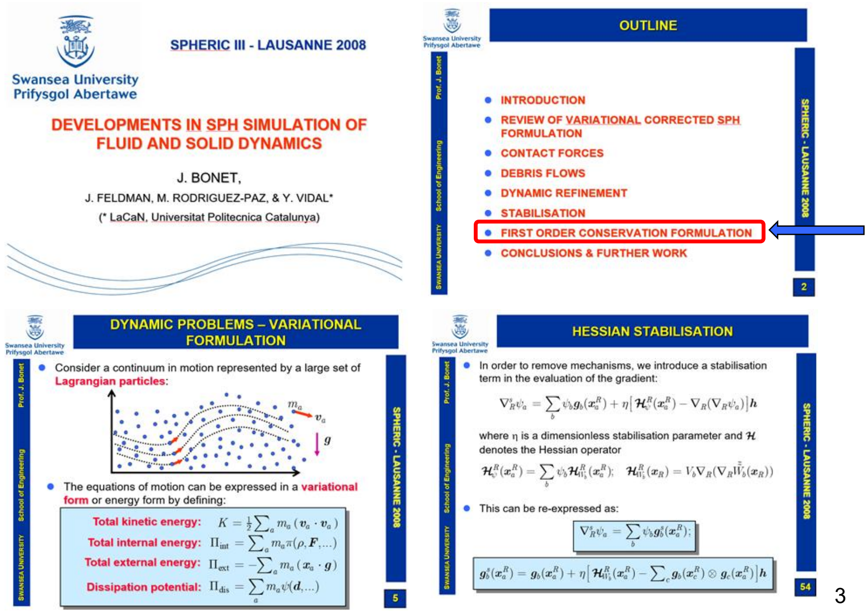

3

CIMNE

MOTIVATION

- Computational Solid Mechanics is a well established and mature subject and there is extensive software available.
- Formulations are usually displacement based where deformation gradient is a function displacement derivatives
- SPH is well established for Free surface flows
- There are various displacement based Updated Lagrangian or total Lagrangian formulations for solid mechanics
- Many stabilisation techniques have emerged in the context of displacement based SPH formulations that eliminate tensile stability and hourglassing
- In the CFD community entropy compliant stabilisation schemes such as upwinding or JST are routine used
- In recent years a new way of formulating solid mechanics as a system of first order conservation laws have been proposed by the authors – this allows the use of CFD stabilisation technology

4

CIMNE®

MOTIVATION - Fracture

- In fracture mechanics experimental and DFT results have shown supersonic and intersonic solutions that cannot be explained by 2nd order displacement based dynamic equations in linear elasticity

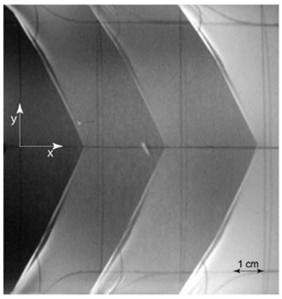

Cracks in rubber under tension exceed the shear wave speed
Paul J. Petersan, Robert D. Deegan, M. Marder, and Harry L. Swinney

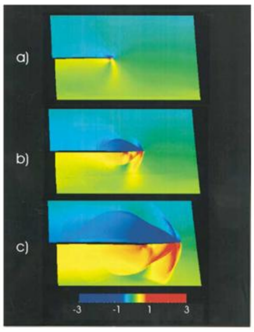

Simulating materials failure …,Farid F. Abraham*†, ...

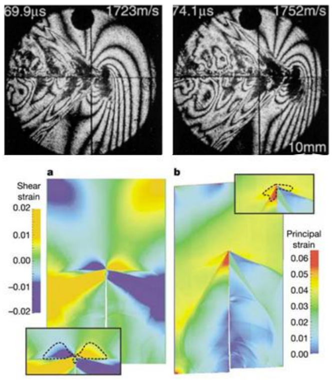

Hyperelasticity governs dynamic fracture at a critical length scale
Markus J. Buehler1*, Farid F. Abraham2* & Huajian Gao1

5

CIMNE®

Aims

- **To derive a mixed formulations for solid dynamics where variables are velocities/displacement AND an extended deformation set that renders the strain energy convex**
- **To derive conservation laws and jump conditions for deformation variables in dynamic applications**
- **To apply the framework to obtain novel analytical intersonic and transonic crack propagation solutions**
- **To use the framework to derive stable and consistent smooth particle hydrodynamic (SPH) formulations for solids**
- **To use this formulation to develop novel approaches for dynamic fracture**

6

Large Deformation Mappings

- Consider a large deformation process:

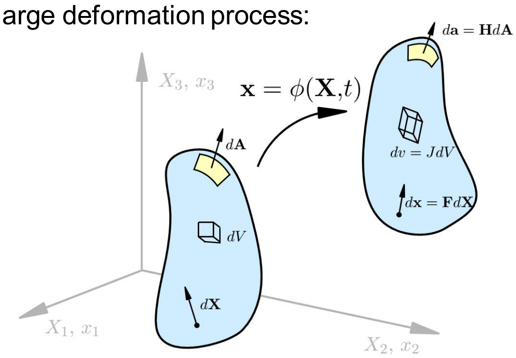

- The fibre, area and volume map are defined by:

$$d\boldsymbol{x} = \boldsymbol{F}d\boldsymbol{X}; \quad \boldsymbol{F} = \boldsymbol{\nabla}_0\boldsymbol{x} = \frac{\partial \boldsymbol{x}}{\partial \boldsymbol{X}}$$
$$d\boldsymbol{a} = \boldsymbol{H}d\boldsymbol{A}; \quad \boldsymbol{H} = \text{Cof}(\boldsymbol{\nabla}_0\boldsymbol{x})$$
$$dv = JdV; \quad J = \det(\boldsymbol{\nabla}_0\boldsymbol{x})$$

Controls Bending

$$\boldsymbol{H} = J\boldsymbol{F}^{-T}$$

7

Tensor Cross Product in Solid Mechanics

- The volume and area map are (3-D):

$$\boldsymbol{H} = \text{Cof}(\boldsymbol{\nabla}_0\boldsymbol{x}) = \tfrac{1}{2}\boldsymbol{\nabla}_0\boldsymbol{x} \times \boldsymbol{\nabla}_0\boldsymbol{x}$$
$$J = \det \boldsymbol{\nabla}_0\boldsymbol{x} = \tfrac{1}{3}\boldsymbol{H} : \boldsymbol{F} = \tfrac{1}{6}\boldsymbol{\nabla}_0\boldsymbol{x} : (\boldsymbol{\nabla}_0\boldsymbol{x} \times \boldsymbol{\nabla}_0\boldsymbol{x})$$

- Where the tensor cross product is:

$$[\boldsymbol{A} \times \boldsymbol{B}]_{iI} = \mathcal{E}_{ijk}\mathcal{E}_{IJK}A_{jJ}B_{kK}$$

$$\boldsymbol{v} \cdot (\boldsymbol{A} \times \boldsymbol{B})\boldsymbol{V} = (\boldsymbol{v} \times \boldsymbol{A}) : (\boldsymbol{B} \times \boldsymbol{V})$$
$$(\boldsymbol{A} \times \boldsymbol{B})(\boldsymbol{V} \times \boldsymbol{W}) = \boldsymbol{A}\boldsymbol{V} \times \boldsymbol{B}\boldsymbol{W} + \boldsymbol{B}\boldsymbol{V} \times \boldsymbol{A}\boldsymbol{W}$$
$$(\boldsymbol{v}_1 \otimes \boldsymbol{V}_1) \times (\boldsymbol{v}_2 \otimes \boldsymbol{V}_2) = (\boldsymbol{v}_1 \times \boldsymbol{v}_2) \otimes (\boldsymbol{V}_1 \times \boldsymbol{V}_2)$$

8

CIMNE

Polyconvex elasticity

- Large strain **polyconvex** strain energy functions $\mathcal{E}$ satisfy (Ball76):

$$\mathcal{E}(\boldsymbol{F},\ldots) = W(\boldsymbol{F},\boldsymbol{H},J,\ldots); \quad W \text{ convex}$$

- Neo-Hookean (or 2-D):

$$W_{NH}(\boldsymbol{F},J) = \tfrac{1}{2}\mu\boldsymbol{F}:\boldsymbol{F} + f(J)$$

- Mooney-Rivlin:

$$W_{MR}(\boldsymbol{F},\boldsymbol{H},J) = \alpha\boldsymbol{F}:\boldsymbol{F} + \beta\boldsymbol{H}:\boldsymbol{H} + f(J)$$

Where: $\alpha + \beta = \dfrac{\mu}{2}$

$$f(J) = \frac{\lambda}{2\varepsilon^2}(J^{\varepsilon} + J^{-\varepsilon}) - 2\alpha\ln J - 4\beta J$$

9

CIMNE

Conjugate Stresses and 1st Piola-Kirchhoff Tensor

- The conjugate stresses to fibre, area and volume maps are:

$$\boldsymbol{\Sigma}_{\boldsymbol{F}} = \frac{\partial W}{\partial \boldsymbol{F}}; \quad \boldsymbol{\Sigma}_{\boldsymbol{H}} = \frac{\partial W}{\partial \boldsymbol{H}}; \quad \Sigma_J = \frac{\partial W}{\partial J}$$

- The relationship between Piola-Kirchhoff and these stresses is:

$$\begin{aligned} D\mathcal{E}(\boldsymbol{F})[\delta\boldsymbol{v}] &= DW(\boldsymbol{F},\boldsymbol{H},J)[\delta\boldsymbol{v}] \\ &= \boldsymbol{\Sigma}_{\boldsymbol{F}} : D\boldsymbol{F}[\delta\boldsymbol{v}] + \boldsymbol{\Sigma}_{\boldsymbol{H}} : D\boldsymbol{H}[\delta\boldsymbol{v}] + \Sigma_J DJ[\delta\boldsymbol{v}] \\ &= \boldsymbol{\Sigma}_{\boldsymbol{F}} : \boldsymbol{\nabla}_0\delta\boldsymbol{v} + \boldsymbol{\Sigma}_{\boldsymbol{H}} : (\boldsymbol{F} \times \boldsymbol{\nabla}_0\delta\boldsymbol{v}) + \Sigma_J\boldsymbol{H} : \boldsymbol{\nabla}_0\delta\boldsymbol{v} \\ &= \left(\boldsymbol{\Sigma}_{\boldsymbol{F}} + \boldsymbol{\Sigma}_{\boldsymbol{H}} \times \boldsymbol{F} + \Sigma_J\boldsymbol{H}\right) : \boldsymbol{\nabla}_0\delta\boldsymbol{v} \\ &= \boldsymbol{P} : \boldsymbol{\nabla}_0\delta\boldsymbol{v} \end{aligned}$$

$$\boldsymbol{P} = \boldsymbol{\Sigma}_{\boldsymbol{F}} + \boldsymbol{\Sigma}_{\boldsymbol{H}} \times \boldsymbol{F} + \Sigma_J\boldsymbol{H}$$

- For Mooney-Rivlin:

$$\boldsymbol{\Sigma}_{\boldsymbol{F}} = 2\alpha\boldsymbol{F}, \qquad \boldsymbol{\Sigma}_{\boldsymbol{H}} = 2\beta\boldsymbol{H}, \qquad \Sigma_J = f'(J)$$

10

CIMNE

Multiphysics - thermoelasticity

- Additional physical effects can be included through energy conjugate pairs. For instance, for thermal effects, entropy is the energy conjugate variable to temperature:

$$\left.\frac{d\mathcal{E}}{dt}\right|_{\boldsymbol{F}=cons} = \theta\dot{\eta} \quad \Rightarrow \quad \theta = \frac{\partial \mathcal{E}(\boldsymbol{F},\eta)}{\partial \eta}$$

- The energy is now a convex multi-variable function as:

$$\mathcal{E}(\boldsymbol{F},\eta) = W(\boldsymbol{F},\boldsymbol{H},J,\eta)$$

- Physical parameters can be used to derive particular functions:

$$\left.\frac{d\mathcal{E}}{d\theta}\right|_{\boldsymbol{F}=cons} = c_V \text{ (specific heat coefficient)}$$

$$\left.\frac{dp}{d\mathcal{E}}\right|_{J=cons} = -\Gamma_0 \text{ (Mie-Gruneisen parameter)}$$

$$W(\boldsymbol{F},\boldsymbol{H},J,\eta) = W_0(\boldsymbol{F},\boldsymbol{H},J) + c_V\theta_R e^{\Gamma_0(1-J)}\left(e^{\eta/c_V} - 1\right)$$

11

CIMNE

Dynamic Conservation Laws

- Consider the **conservation of linear momentum:**

$$\frac{d}{dt}\int_{\Omega_0} \rho_0 \boldsymbol{v}\, dV = \int_{\Omega_0} \boldsymbol{f}_0\, dV + \int_{\partial\Omega_0} \boldsymbol{t}_0\, dA; \qquad \boldsymbol{t}_0 = \boldsymbol{PN}$$

- In differential form:

$$\frac{\partial \boldsymbol{p}}{\partial t} - DIV\boldsymbol{P} = \boldsymbol{f}_0 \; ; \quad \boldsymbol{p} = \rho_0 \boldsymbol{v}$$

- Conservation of Energy (first law of thermodynamics):

$$\frac{d}{dt}\int_{\Omega_0} E\, dV = \int_{\Omega_0} (r_0 + \boldsymbol{v}\cdot\boldsymbol{f}_0)\, dV + \int_{\partial\Omega_0} (\boldsymbol{v}\cdot\boldsymbol{t}_0 - Q_N)\, dA$$

$$\frac{\partial E}{\partial t} + DIV(\boldsymbol{Q} - \boldsymbol{P}^T\boldsymbol{v}) = r_0 + \boldsymbol{v}\cdot\boldsymbol{f}_0; \quad E = \frac{1}{2\rho_0}\boldsymbol{p}\cdot\boldsymbol{p} + \mathcal{E}$$

$$\frac{\partial \eta}{\partial t} + DIV\left(\frac{\boldsymbol{Q}}{\theta}\right) = s_0; \quad s_0 = \frac{r_0}{\theta} + \frac{D_{\text{int}}}{\theta} - \frac{1}{\theta^2}\boldsymbol{Q}\cdot\nabla_0\theta$$

12

CIMNE

Geometric Conservation Laws

- Conservation of deformation gradient:

$$\boldsymbol{F} = \boldsymbol{\nabla}_0 \phi \Rightarrow \int_{\Omega_0} \boldsymbol{F}\, dV = \int_{\partial\Omega_0} \phi \otimes d\boldsymbol{A}$$

$$\Rightarrow \frac{d}{dt} \int_{\Omega_0} \boldsymbol{F}\, dV = \int_{\partial\Omega_0} \boldsymbol{v} \otimes d\boldsymbol{A}$$

$$\frac{\partial \boldsymbol{F}}{\partial t} - DIV(\boldsymbol{v} \otimes \boldsymbol{I}) = \boldsymbol{0}$$

- Conservation of volume map:

$$\frac{d}{dt} \int_{\Omega} dv = \int_{\partial\Omega} \boldsymbol{v} \cdot d\boldsymbol{a} \Rightarrow \frac{d}{dt} \int_{\Omega_0} J\, dV = \int_{\partial\Omega_0} \boldsymbol{H} : (\boldsymbol{v} \otimes d\boldsymbol{A})$$

$$\frac{\partial J}{\partial t} - DIV(\boldsymbol{H}^T \boldsymbol{v}) = 0$$

13

CIMNE

Conservation of Area Map

- Using the tensor cross product:

$$\boldsymbol{H} = \tfrac{1}{2} \boldsymbol{F} \times \boldsymbol{F}; \quad \Rightarrow \quad \frac{\partial \boldsymbol{H}}{\partial t} = \boldsymbol{F} \times \boldsymbol{\nabla}_0 \boldsymbol{v} = CURL(\boldsymbol{v} \times \boldsymbol{F})$$

- Where the material curl is:

$$[CURL(\boldsymbol{A})]_{iI} = \mathcal{E}_{IJK} \frac{\partial A_{iK}}{\partial X_J}$$

- A conservation law emerges as:

$$\frac{\partial \boldsymbol{H}}{\partial t} - CURL(\boldsymbol{v} \times \boldsymbol{F}) = \boldsymbol{0}$$

$$\frac{d}{dt} \int_{\Omega_0} \boldsymbol{H}\, dV = \int_{\partial\Omega_0} \boldsymbol{F} \times (\boldsymbol{v} \otimes d\boldsymbol{A})$$

14

Conservation laws for Solid Dynamics

- The complete set of conservation laws is:

$$\frac{\partial \boldsymbol{p}}{\partial t} - DIV\boldsymbol{P} = \boldsymbol{f}_0$$
$$\frac{\partial \boldsymbol{F}}{\partial t} - DIV(\boldsymbol{v} \otimes \boldsymbol{I}) = \boldsymbol{0}$$
$$\frac{\partial \boldsymbol{H}}{\partial t} - CURL(\boldsymbol{v} \times \boldsymbol{F}) = \boldsymbol{0}$$
$$\frac{\partial J}{\partial t} - DIV(\boldsymbol{H}^T \boldsymbol{v}) = 0$$
$$\frac{\partial \eta}{\partial t} + DIV(\frac{\boldsymbol{Q}}{\theta}) = s_0$$

- And constitutive model

$$\boldsymbol{v} = \frac{1}{\rho_0}\boldsymbol{p}; \quad \boldsymbol{P} = \boldsymbol{P}(\boldsymbol{F}, H, J, \ldots); \quad \boldsymbol{Q} = \boldsymbol{Q}(\boldsymbol{\nabla}_0 \theta); \quad \theta = \theta(\eta, \boldsymbol{F}, \ldots)$$

15

System of conservation laws

- Using the combined notation:

$$\boldsymbol{\mathcal{U}} = \begin{bmatrix} \boldsymbol{p} \\ \boldsymbol{F} \\ H \\ J \\ \eta \end{bmatrix}; \quad \boldsymbol{\mathcal{F}}_I = -\begin{bmatrix} \boldsymbol{P}\boldsymbol{E}_I \\ \boldsymbol{v} \otimes \boldsymbol{E}_I \\ F \times (v \otimes E_I) \\ \boldsymbol{H} : (\boldsymbol{v} \otimes \boldsymbol{E}_I) \\ Q_I / \theta \end{bmatrix}; \quad \boldsymbol{E}_{1,2,3} = \begin{bmatrix} 1 \\ 0 \\ 0 \end{bmatrix}, \begin{bmatrix} 0 \\ 1 \\ 0 \end{bmatrix}, \begin{bmatrix} 0 \\ 0 \\ 1 \end{bmatrix}$$

- The system can be expressed in standard form with jump conditions:

$$\boldsymbol{\mathcal{R}} = \frac{\partial \boldsymbol{\mathcal{U}}}{\partial t} + \frac{\partial \boldsymbol{\mathcal{F}}_I}{\partial X_I} - \boldsymbol{\mathcal{S}} = \boldsymbol{0}; \quad \boldsymbol{\mathcal{S}} = \begin{bmatrix} \boldsymbol{f}_0 \\ \boldsymbol{0} \\ \boldsymbol{0} \\ 0 \\ s_0 \end{bmatrix}$$

$$U [\![\boldsymbol{\mathcal{U}}]\!] = [\![\boldsymbol{\mathcal{F}}_N]\!]$$

16

ALE & URTL Formulations

- Through integral transformations and Reynolds transport theorem:

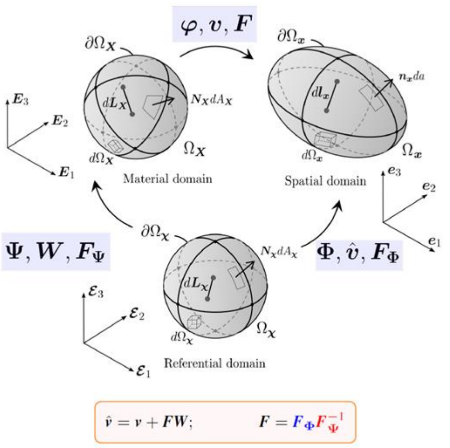

$$\frac{\partial J_\Psi \boldsymbol{p}}{\partial t} - DIV_\chi\left[(\boldsymbol{P} + \boldsymbol{p} \otimes \boldsymbol{W})\boldsymbol{H}_\Psi\right] = J_\Psi \boldsymbol{f}_0$$
$$\frac{\partial \boldsymbol{F}_\Phi}{\partial t} - DIV_\chi(\hat{\boldsymbol{v}} \otimes \boldsymbol{I}) = \boldsymbol{0}$$
$$\frac{\partial \boldsymbol{F}_\Psi}{\partial t} - DIV_\chi(\boldsymbol{W} \otimes \boldsymbol{I}) = \boldsymbol{0}$$
$$\frac{\partial J_\Psi \rho_0}{\partial t} - DIV_\chi(\rho_0 \boldsymbol{H}_\Psi^T \boldsymbol{W}) = 0$$
$$\frac{\partial J_\Psi \eta}{\partial t} - DIV_\chi\left(\eta \boldsymbol{H}_\Psi^T \boldsymbol{W} - \frac{\boldsymbol{Q}_\chi}{\theta}\right) = J_\Psi s_0$$

Includes, Updated reference Lagrangian formulation (URL), particle shifting and velocity shifting formulations

C. H. Lee, A. J. Gil, P. R. R. de Campos, J. Bonet, T. Jaugielavicius, S. Joshi and C. Wood, *A Novel ALE SPH Algorithm for Nonlinear Solid Dynamics*, CMAME 2024.

Conservation laws in linear elasticity

- In linear elasticity the set of 1st order conservation laws is:

$$\frac{\partial \boldsymbol{p}}{\partial t} - \operatorname{div} \boldsymbol{\sigma} = \boldsymbol{f}$$
$$\frac{\partial \boldsymbol{G}}{\partial t} - \operatorname{div}(\boldsymbol{v} \otimes \boldsymbol{I}) = \boldsymbol{0}$$

$$\boldsymbol{v} = \frac{1}{\rho}\boldsymbol{p} = \dot{\boldsymbol{u}};$$
$$\boldsymbol{\sigma} = \lambda \operatorname{tr} \boldsymbol{G} + \mu(\boldsymbol{G} + \boldsymbol{G}^T);$$
$$\boldsymbol{G} = \nabla \boldsymbol{u}$$

- With jump conditions:

$$\rho c [\![\boldsymbol{v}]\!] = -[\![\boldsymbol{\sigma}]\!] \boldsymbol{n}$$
$$c [\![\boldsymbol{G}]\!] = -[\![\boldsymbol{v}]\!] \otimes \boldsymbol{n}$$

$$c = \begin{cases} c_p = \sqrt{\frac{\lambda + 2\mu}{\rho}} & [\![\boldsymbol{v}]\!] = [\![v_n]\!] \boldsymbol{n} \\ c_s = \sqrt{\frac{\mu}{\rho}} & [\![\boldsymbol{v}]\!] = [\![v_s]\!] \boldsymbol{\nu} \end{cases}$$

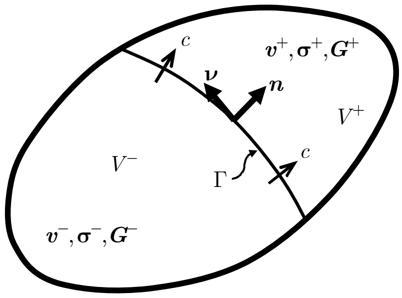

18

CIMNE

Dynamic crack propagation – 1- D

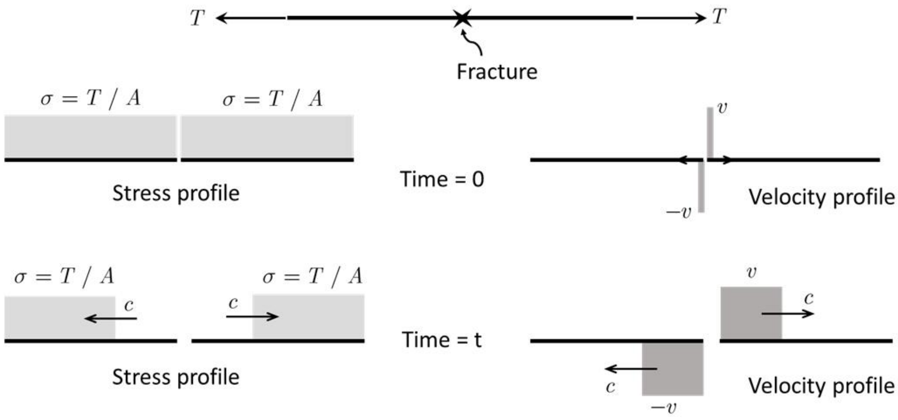

$$v = \frac{\sigma}{\rho c}; \quad c = \sqrt{\frac{E}{\rho}}; \quad K = \mathcal{E} = \tfrac{1}{2}\rho v^2 = \tfrac{1}{2E}\sigma^2$$

19

CIMNE

Dynamic crack propagation – mode I

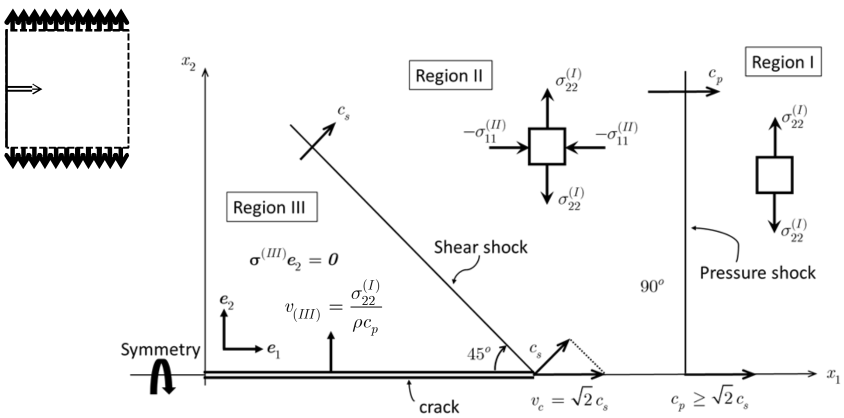

BONET, J., GIL, A.J., *Mathematical models of supersonic and intersonic crack propagation in linear elastodynamics*, *International Journal of Fracture*, 229 (1), pp. 55-75., 2021.

20

CIMNE

Dynamic crack propagation – mode II

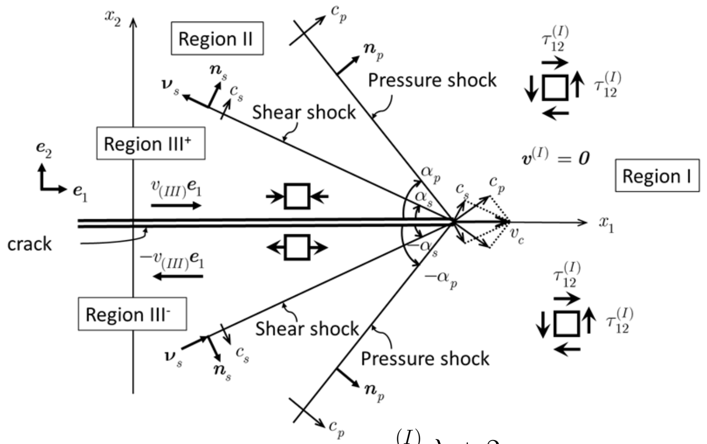

$$\alpha_p = 2\alpha_s;$$
$$\cos\alpha_s = c_p / 2c_s$$

$$\boldsymbol{v}^{(III)} = \pm \frac{\tau_{12}^{(I)}}{\rho c_p}\frac{\lambda + 2\mu}{\lambda}\boldsymbol{e}_1;$$

$$\boldsymbol{\sigma}^{(III)} = \pm 2\tau_{12}^{(I)}\frac{\lambda + \mu}{\lambda}\sqrt{\frac{2\mu - \lambda}{2\mu + \lambda}}\,\boldsymbol{e}_1 \otimes \boldsymbol{e}_1;$$

21

CIMNE

System of conservation laws

- Using the combined notation:

$$\boldsymbol{\mathcal{U}} = \begin{bmatrix} \boldsymbol{p} \\ \boldsymbol{F} \\ \boldsymbol{H} \\ J \\ \eta \end{bmatrix}; \quad \boldsymbol{\mathcal{F}}_I = -\begin{bmatrix} \boldsymbol{P}\boldsymbol{E}_I \\ \boldsymbol{v} \otimes \boldsymbol{E}_I \\ \boldsymbol{F} \times (\boldsymbol{v} \otimes \boldsymbol{E}_I) \\ \boldsymbol{H} : (\boldsymbol{v} \otimes \boldsymbol{E}_I) \\ Q_I \,/\, \theta \end{bmatrix}; \quad \boldsymbol{E}_{1,2,3} = \begin{bmatrix} 1 \\ 0 \\ 0 \end{bmatrix}, \begin{bmatrix} 0 \\ 1 \\ 0 \end{bmatrix}, \begin{bmatrix} 0 \\ 0 \\ 1 \end{bmatrix}$$

- The system can be expressed in standard form with jump conditions:

$$\boldsymbol{\mathcal{R}} = \frac{\partial \boldsymbol{\mathcal{U}}}{\partial t} + \frac{\partial \boldsymbol{\mathcal{F}}_I}{\partial X_I} - \boldsymbol{\mathcal{S}} = \boldsymbol{0}; \quad \boldsymbol{\mathcal{S}} = \begin{bmatrix} \boldsymbol{f}_0 \\ \boldsymbol{0} \\ \boldsymbol{0} \\ 0 \\ s_0 \end{bmatrix}$$

$$U[\![\boldsymbol{\mathcal{U}}]\!] = [\![\boldsymbol{\mathcal{F}}_N]\!]$$

22

Convex entropy extension - Stability

- The system has a **convex entropy extension** function and associated fluxes such that (Wagner):

$$\frac{\partial S}{\partial t}+\frac{\partial \Lambda_I}{\partial X_I}\leq 0$$

- For thermo-elastic problems S is the "**ballistic free energy**" *B*:

$$B(\boldsymbol{\mathcal{U}})=E-\theta_R\eta=\tfrac{1}{2\rho_0}\boldsymbol{p}\cdot\boldsymbol{p}+W(\boldsymbol{F},\boldsymbol{H},J,\eta)-\theta_R\eta;$$

$$\Lambda_I=\frac{\Delta\theta}{\theta}Q_I-\boldsymbol{P}:(\boldsymbol{v}\otimes\boldsymbol{E}_I);\qquad \boldsymbol{\mathcal{V}}=\frac{\partial B}{\partial \boldsymbol{\mathcal{U}}}=\left\{\boldsymbol{v},\boldsymbol{\Sigma}_F,\boldsymbol{\Sigma}_H,\Sigma_J,\Delta\theta\right\}$$

- Globally:

$$\frac{d}{dt}\int_V B\,dV-\dot{\Pi}_{\text{ext}}-\mathcal{Q}_{\text{ext}}\leq 0$$

$$\dot{\Pi}_{\text{ext}}=\int_V \boldsymbol{f}_0\cdot\boldsymbol{v}\,dV+\int_{\partial V}\boldsymbol{t}_B\cdot\boldsymbol{v}\,dA;\quad \mathcal{Q}_{\text{ext}}=\int_V\frac{\Delta\theta}{\theta}r_0\,dV-\int_{\partial V}\frac{\Delta\theta}{\theta}Q_B\,dA$$

23

Weak form conservation laws

- Using conjugate variables the weak form of conservation laws are:

$$\int_V \delta\boldsymbol{\mathcal{V}}^T\dot{\boldsymbol{\mathcal{U}}}\,dV=\int_V\delta\boldsymbol{\mathcal{V}}^T\boldsymbol{\mathcal{S}}\,dV+\int_{\partial V}\frac{\partial\delta\boldsymbol{\mathcal{V}}^T}{\partial X_I}\boldsymbol{\mathcal{F}}_I\,dA-\int_{\partial V}\delta\boldsymbol{\mathcal{V}}^T\boldsymbol{\mathcal{F}}_N\,dA$$

- Which in component form is:

$$\int_V\delta\boldsymbol{v}\cdot\dot{\boldsymbol{p}}\,dV=-\int_V\boldsymbol{P}:\nabla_0\delta\boldsymbol{v}\,dV\int_V\delta\boldsymbol{v}\cdot\boldsymbol{f}_0\,dV+\int_{\partial V}\delta\boldsymbol{v}\cdot\boldsymbol{t}_B\,dA$$

$$\int_V\delta\boldsymbol{\Sigma}_F:\dot{\boldsymbol{F}}\,dV=\int_V\delta\boldsymbol{\Sigma}_F\cdot\nabla_0\delta\boldsymbol{v}\,dV$$

$$\int_V\delta\boldsymbol{\Sigma}_H:\dot{\boldsymbol{H}}\,dV=\int_V\delta\boldsymbol{\Sigma}_H\cdot(\boldsymbol{F}\times\nabla_0\delta\boldsymbol{v})\,dV$$

$$\int_V\delta\Sigma_J\dot{J}\,dV=\int_V\delta\Sigma_J\boldsymbol{H}:(\nabla_0\delta\boldsymbol{v})\,dV$$

$$\int_V\delta\theta\dot{\eta}\,dV=\int_V\frac{\boldsymbol{Q}}{\theta}:\nabla_0\delta\theta\,dV-\int_V\delta\theta\left(\frac{r_0}{\theta}-\frac{1}{\theta^2}\boldsymbol{Q}\cdot\nabla_0\theta\right)dV$$

$$-\int_{\partial V}\delta\theta\frac{Q_B}{\theta_B}\,dA$$

24

Corrected SPH Discretisation

- We use a corrected SPH discretisation using kernel functions *W* such that function gradients are:

$$\nabla_0 \varphi\big|_a \simeq \sum_{b\in\Lambda_a^b} V_b(\varphi_b - \varphi_a)\tilde{\nabla}_0 W_b(\boldsymbol{X}_a)$$
$$\tilde{\nabla}_0 W_b(X_a) = \boldsymbol{L}_a \nabla_0 W_b(\boldsymbol{X}_a)$$
$$\boldsymbol{L}_a = \left[\sum_{b\in\Lambda_a^b} V_b(\boldsymbol{X}_b - \boldsymbol{X}_a)\otimes\nabla_0 W_b(X_a)\right]^{-T}$$

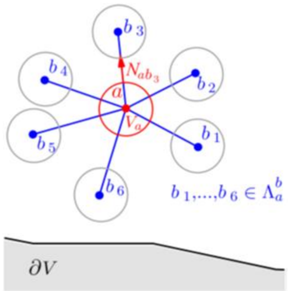

- In order to mirror vertex centre FV methods this is written as:

$$\nabla_0 \varphi\big|_a \simeq \frac{1}{V_b}\sum_{b\in\Lambda_a^b} \tfrac{1}{2}(\varphi_b - \varphi_a)\boldsymbol{C}_{ab}$$
$$\boldsymbol{C}_{ab} = 2V_a V_b \tilde{\nabla}_0 W_b(X_a);\quad \boldsymbol{C}_{ab} \neq -\boldsymbol{C}_{ba}$$

25

CSPH semi-discrete equations

- Using particle integration and CSPH evaluation of gradients gives:

$$V_a\dot{\boldsymbol{p}}_a = \sum_{b\in\Lambda_a^b}\tfrac{1}{2}\left(\boldsymbol{P}_a\boldsymbol{C}_{ab} - \boldsymbol{P}_b\boldsymbol{C}_{ba}\right) + V_a\boldsymbol{f}_0 + A_a\boldsymbol{t}_a^B + \sum_{b\in\Lambda_a^b}\boldsymbol{D}_{ab}^v$$
$$V_a\dot{\boldsymbol{F}}_a = \sum_{b\in\Lambda_a^b}\tfrac{1}{2}\left(\boldsymbol{v}_b - \boldsymbol{v}_a\right)\otimes\boldsymbol{C}_{ab}$$
$$V_a\dot{\boldsymbol{H}}_a = \boldsymbol{F}_a \times \sum_{b\in\Lambda_a^b}\tfrac{1}{2}\left(\boldsymbol{v}_b - \boldsymbol{v}_a\right)\otimes\boldsymbol{C}_{ab}$$
$$V_a\dot{J}_a = \boldsymbol{H}_a : \sum_{b\in\Lambda_a^b}\tfrac{1}{2}\left(\boldsymbol{v}_b - \boldsymbol{v}_a\right)\otimes\boldsymbol{C}_{ab} + \sum_{b\in\Lambda_a^b} D_{ab}^J$$
$$V_a\dot{\eta}_a = \sum_{b\in\Lambda_a^b}\tfrac{1}{2}\left(\frac{\boldsymbol{Q}_b}{\theta_b}\boldsymbol{C}_{ba} - \frac{\boldsymbol{Q}_a}{\theta_a}\boldsymbol{C}_{ab}\right) - \frac{\boldsymbol{Q}_a}{\theta_a^2}\cdot\sum_{b\in\Lambda_a^b}\tfrac{1}{2}\left(\theta_b - \theta_a\right)\boldsymbol{C}_{ab}$$
$$+V_a\frac{r_0}{\theta_a} - \frac{Q_B}{\theta_a^B}A_a$$

26

CIMNE

SPH Stabilisation

- Multiplying semi-discrete equations by conjugate variables and adding:

$$\frac{d}{dt}\sum_a V_a B_a - \dot{\Pi}_{\text{ext}} - \mathcal{Q}_{\text{ext}} = \sum_a V_a \frac{\theta_R}{\theta_a^2}\boldsymbol{Q}_a \cdot \nabla_0 \theta(\boldsymbol{X}_a) - \sum_{a,b\in\Lambda_a^b} \tfrac{1}{2}\left(\boldsymbol{v}_b - \boldsymbol{v}_a\right)\cdot \boldsymbol{D}^v_{ab} - \sum_{a,b\in\Lambda_a^b} \tfrac{1}{2}\left(\Sigma_J^b - \Sigma_J^a\right) D^J_{ab} \leq 0$$

- Stability is ensured if:

$$\boldsymbol{D}^v_{ab} = \boldsymbol{S}^v_{ab}\left(\boldsymbol{v}_b - \boldsymbol{v}_a\right); \qquad D^J_{ab} = S^J_{ab}(\Sigma_J^b - \Sigma_J^a)$$

$$\boldsymbol{S}^v_{ab} = \tfrac{1}{2}\rho\left\|\bar{\boldsymbol{C}}_{ab}\right\|\left[c_p \boldsymbol{n}_{ab}\otimes\boldsymbol{n}_{ab} + c_s(\boldsymbol{I} - \boldsymbol{n}_{ab}\otimes\boldsymbol{n}_{ab})\right];$$

$$S^J_{ab} = \frac{\left\|\bar{\boldsymbol{H}}_{ab}\bar{\boldsymbol{C}}_{ab}\right\|^2}{2\rho c_p\left\|\bar{\boldsymbol{C}}_{ab}\right\|}$$

27

CIMNE

Discrete Fracture modelling

- As a particle reaches fracture criterium (maximum principal stress)

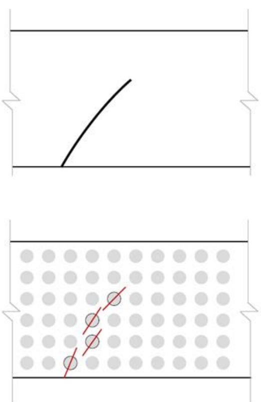

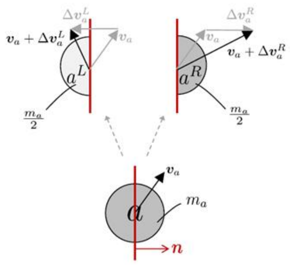

$$\left[\!\left[\boldsymbol{F}\right]\!\right] = \boldsymbol{F}_a^+ - \boldsymbol{F}_a = -\boldsymbol{\beta}_a \otimes \boldsymbol{N}_X;$$

$$\boldsymbol{P}_a^+(\boldsymbol{F}_a - \boldsymbol{\beta}_a \otimes \boldsymbol{N}_X)\boldsymbol{N}_X = \boldsymbol{0}$$

$$\Delta\boldsymbol{v}_a = \Delta v_a \boldsymbol{n}_a$$

$$\tfrac{1}{2}\rho_X^a\left(\Delta v_a\right)^2 = \mathcal{E}(\boldsymbol{F}_a) - \mathcal{E}(\boldsymbol{F}_a^+)$$

28

TIME INTEGRATION

- Integration in time is achieved by means of an explicit Total Variational Diminishing (TVD) Runge-Kutta scheme:

$$\mathcal{U}^{(1)}_{n+1} = \mathcal{U}_n + \Delta t \dot{\mathcal{U}}_n$$
$$\mathcal{U}^{(2)}_{n+2} = \mathcal{U}^{(1)}_{n+1} + \Delta t \dot{\mathcal{U}}^{(1)}_{n+1}$$
$$\mathcal{U}_{n+1} = \tfrac{1}{2}\mathcal{U}_n + \tfrac{1}{2}\mathcal{U}^{(2)}_{n+2}$$

with a stability constraint:

$$\Delta t = CFL \frac{h_{\min}}{U^n_{\max}}$$

- Geometry increment:

$$\boldsymbol{x}_{n+1} = \boldsymbol{x}_n + \frac{\Delta t}{2}(\boldsymbol{v}_n + \boldsymbol{v}_{n+1})$$

29

3D SWINGING PLATE I

Problem description: Unit solid cube, $\rho_0 = 1.1 \times 10^3 kg/m^3$, $E = 1.7 \times 10^7 Pa$, $\nu = 0.45$, $\alpha_{CFL} = 0.3$, $U_0 = 5 \times 10^{-4}$, $\tau_F = 0.5\,\Delta t$, $\tau_p = \alpha = 0$, $A = B = 1$, $C = -2$, lumped mass matrix

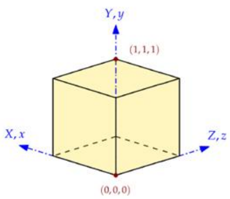

$$\boldsymbol{u} = U_0 \cos\left(\frac{\sqrt{3}}{2} c_d \pi t\right) \begin{bmatrix} A \sin\left(\frac{\pi X_1}{2}\right) \cos\left(\frac{\pi X_2}{2}\right) \cos\left(\frac{\pi X_3}{2}\right) \\ B \cos\left(\frac{\pi X_1}{2}\right) \sin\left(\frac{\pi X_2}{2}\right) \cos\left(\frac{\pi X_3}{2}\right) \\ C \cos\left(\frac{\pi X_1}{2}\right) \cos\left(\frac{\pi X_2}{2}\right) \sin\left(\frac{\pi X_3}{2}\right) \end{bmatrix}$$

Linear momentum

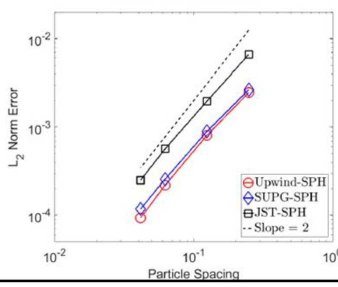

Stresses

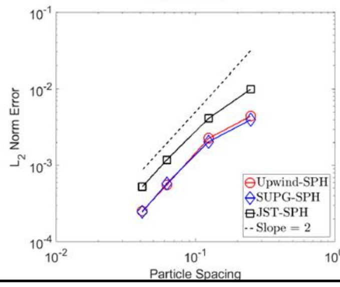

CIMNE

L-Shape rotation

Problem: **L-shaped block**, neo-Hookean model, $\rho_R = 1000$ kg/m^3, $E = 50.5$ kPa, $\nu = 0.3$.

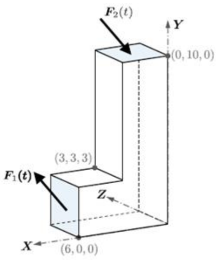

$$F_1(t) = -F_2(t) = (150, 300, 450)^T\, p(t);$$

$$p(t) = \begin{cases} t & 0 \le t < 2.5 \\ 5 - t & 2.5 \le t < 5 \\ 0 & t \ge 5 \end{cases}$$

[L-shaped block]

Video

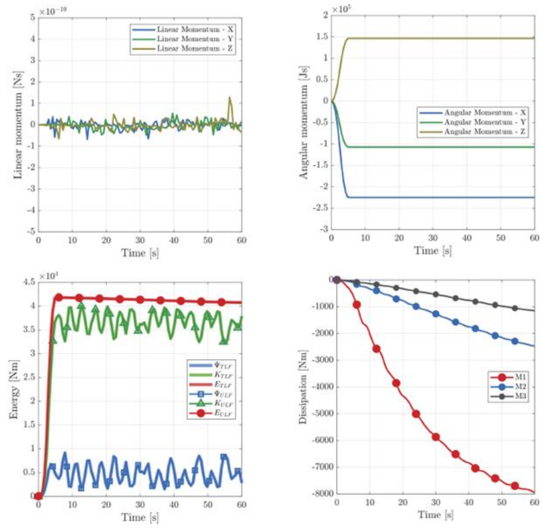

CIMNE

3D TWISTING COLUMN – COMPARISON

Problem: **Twisting column**, neo-Hookean model, $\rho_R = 1100$ kg/m^3, $E = 17$ MPa, $\nu = 0.495$.

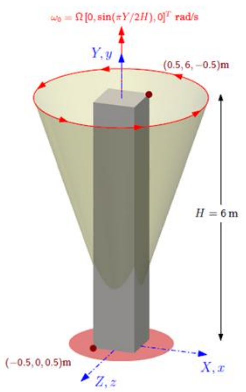

[Twisting column]

Video

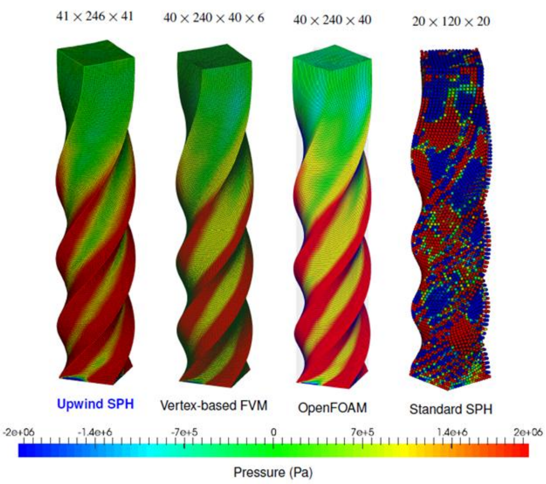

CIMNE 3D TWISTING COLUMN – ST VENANT

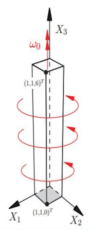

$$v^0 = \omega \times X; \qquad \omega = \left(0, 0, 100 \sin\left(\frac{\pi X_3}{2L}\right)\right)^T$$

Highly **localised** deformation

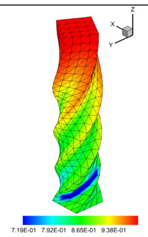

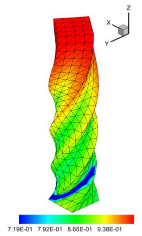

Negative acoustic tensor

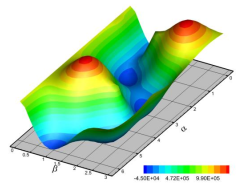

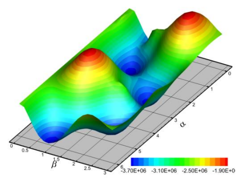

MOX-Milan 2019

33

CIMNE Assessment of ALE equations- Patch test

- **Patch test:** $\rho_R = 1100$ kg/m^3, $E = 17$ MPa, Poisson's ratio $\nu = 0.45$, initial velocity $v_0 = [1, 1, 0]^T$, $\beta = 0.02$, $H = 6$ m, $L = 1$ m, $T = 0.5$ s. Finite Volume Method.

[Patch test]

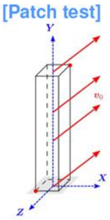

Prescribed material motion:

$$u_\Psi = \begin{bmatrix} \beta \sin^2\left(\frac{\pi t}{T}\right) \sin\left(\frac{2\pi \chi_1}{L}\right) \left[\cos\left(\frac{2\pi \chi_2}{H}\right) + \sin\left(\frac{2\pi \chi_2}{H}\right)\right] \\ 5\beta \sin^2\left(\frac{2\pi t}{T}\right) \sin\left(\frac{2\pi \chi_2}{H}\right) \left[\cos\left(\frac{2\pi \chi_1}{L}\right) + \sin\left(\frac{2\pi \chi_1}{L}\right)\right] \\ 0 \end{bmatrix}$$

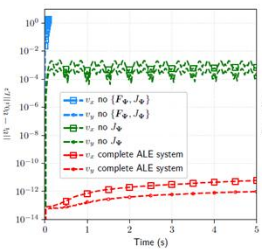

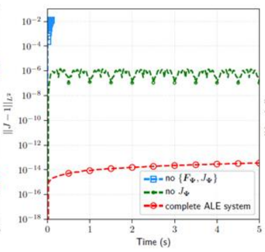

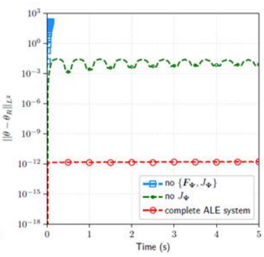

34

Assessment of ALE equations-Convergence

· **Large strain:** neo-Hookean, $\rho_R = 1100$ kg/m^3, $E = 17$ MPa, Poisson's ratio $\nu = 0.45$, $v_0 = 1$m/s, $\beta = 0.02$ and $T = 0.5$ s. SPH method.

Prescribed material particle motion:

$$u_\Psi = \begin{bmatrix} \beta \sin^2\left(\frac{\pi t}{T}\right) \sin\left(\frac{2\pi \chi_1}{L}\right) \left[\cos\left(\frac{2\pi \chi_2}{H}\right) + \sin\left(\frac{2\pi \chi_2}{H}\right)\right] \\ 5\beta \sin^2\left(\frac{2\pi t}{T}\right) \sin\left(\frac{2\pi \chi_2}{H}\right) \left[\cos\left(\frac{2\pi \chi_1}{L}\right) + \sin\left(\frac{2\pi \chi_1}{L}\right)\right] \\ 0 \end{bmatrix}$$

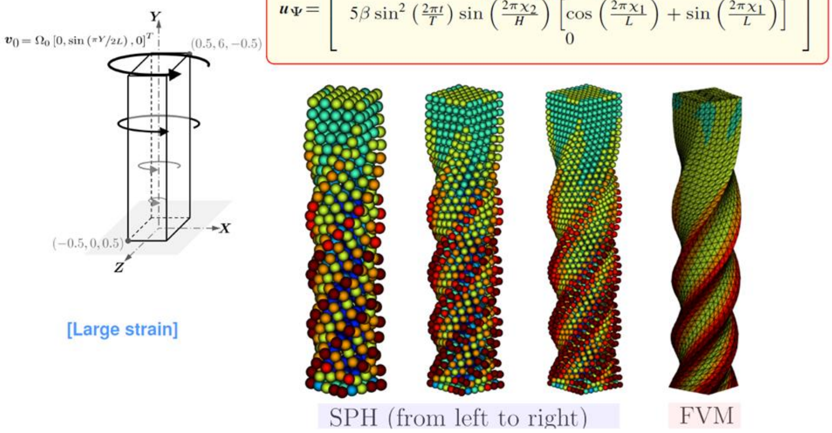

Taylor Test

Taylor bar: von-Mises plasticity, $\rho_R = 8930$kg/m^3, $E = 124$ GPa, Poisson's ratio $\nu = 0.34$, yield stress $\bar{\tau}_y^0 = 90$ MPa, hardening parameter $H = 292$ MPa. SPH method. [Impact]

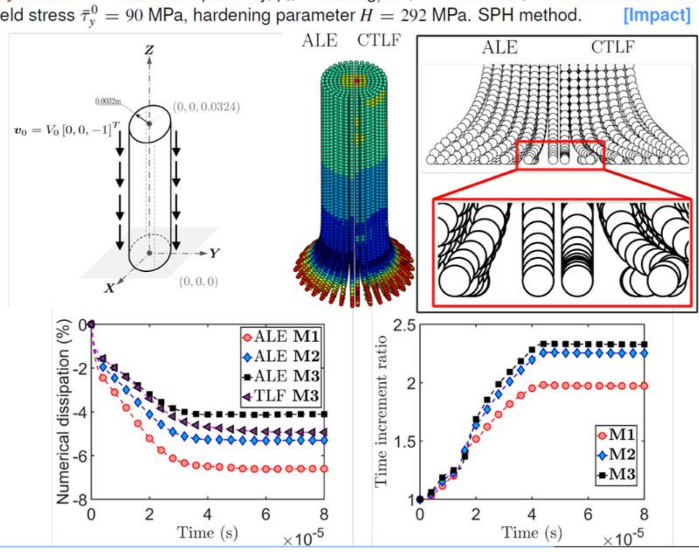

Coining Test

Large plastic flow: Hencky-based von-Mises plasticity, $\rho_R = 8930 \text{kg/m}^3$, $E = 1$ MPa, Poisson's ratio $\nu = 0.3$, yield stress $\bar{\tau}_y^0 = 250$ Pa, hardening parameter $H = 1000$ Pa. Velocity $V_0 = 10$ m/s. Time $t_0 = 6e^{-4}$. Material mesh motion via conservation type of law.

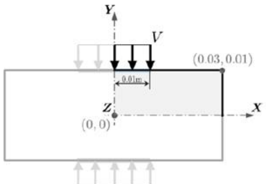

$$V(t) = \begin{cases} \frac{V_0 t}{t_0} & t \leq t_0 \\ V_0 & \text{otherwise} \end{cases}$$

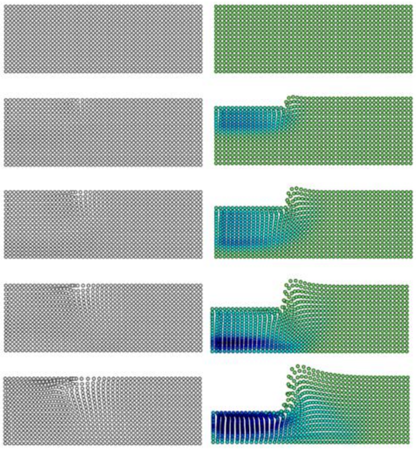

[Coining]

Video

37

Dynamic Fracture

Problem: **Mixed-mode dynamic fracture**, linear elastic model, $\rho_R = 2400$ kg/m^3, $E = 31.37$ GPa, $\nu = 0.2$, maximum principal stress $\sigma_0^{\max} = 10.45$ MPa, fracture energy $G_f = 19.58$ N/m, $t_0 = 1.96 \times 10^{-4}$s and $V_0 = 0.06$ ms^{-1}.

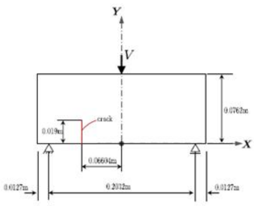

$$V(t) = \begin{cases} \frac{V_0 t}{t_0} & t \leq t_0 \\ V_0 & \text{otherwise} \end{cases}$$

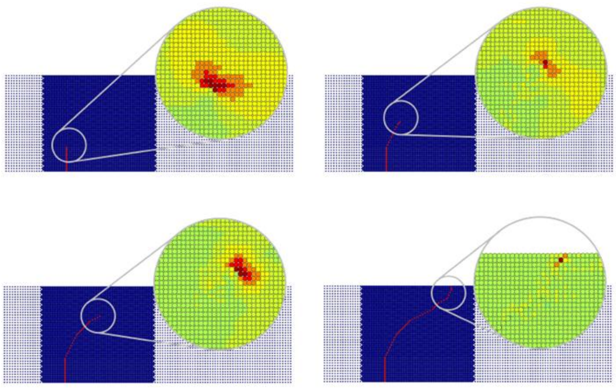

[Beam impact] Video

Dynamic Fracture

Problem: **Notched plate with hole**, linear elastic model, $\rho_R = 2000$ kg/m^3, $E = 59.83$ GPa, $\nu = 0.22$, maximum admissible principal stress $\sigma_0^{\text{max}} = 80$ MPa, and $V = 0.5$ ms^{-1}.

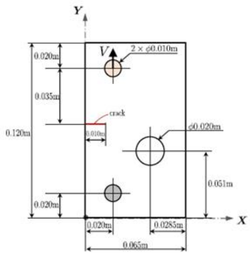

[Notched plate]

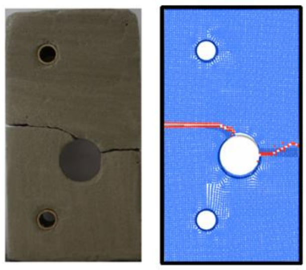

A review on phase-field models of brittle fracture and a new fast hybrid formulation

Marreddy Ambati · Tymofiy Gerasimov · Laura De Lorenzis

Dynamic Fracture

- **Problem description** Linear elasticity, $\rho_R = 2450$ kg m^{-3}, $E = 32$ GPa, Poisson's ratio $\nu = 0.2$, maximum principal stress $S_{\text{max}} = 7.3485$ MPa. A traction $\boldsymbol{t} = [0, t_y]^T$ is applied over time. Two loading scenarios are considered: (1) step function in t_y, and (2) a smooth function characterised by the parameter $t_0 = 0.515\ \mu s$.

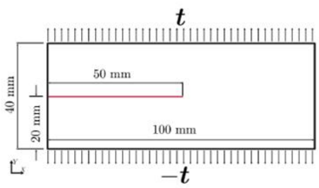

$$t_y = \begin{cases} 1\ \text{MPa} \cdot t/t_0 & t < t_0 \\ 1\ \text{MPa} & t \geq t_0 \end{cases}$$

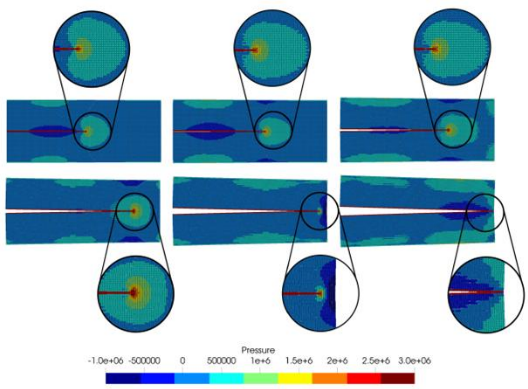

CIMNE

Dynamic Fracture

- **Problem description** Linear elasticity, $\rho_R = 2450$ kg m^{-3}, $E = 32$ GPa, Poisson's ratio $\nu = 0.2$, maximum principal stress $S_{\max} = 7.3485$ MPa. A traction $\boldsymbol{t} = [0, t_y]^T$ is applied over time. Two loading scenarios are considered: (1) step function in t_y, and (2) a smooth function characterised by the parameter $t_0 = 0.515\ \mu s$.

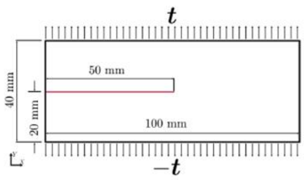

$t_y = 1$MPa; $t \geq 0$

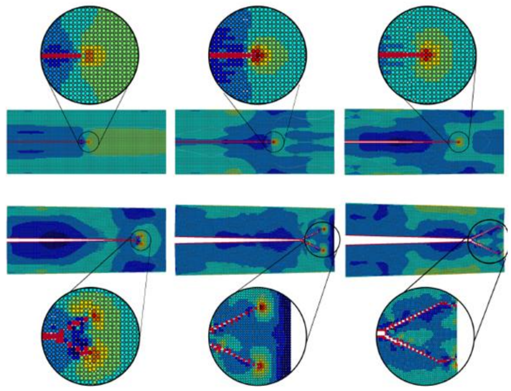

CIMNE

Dynamic Fracture

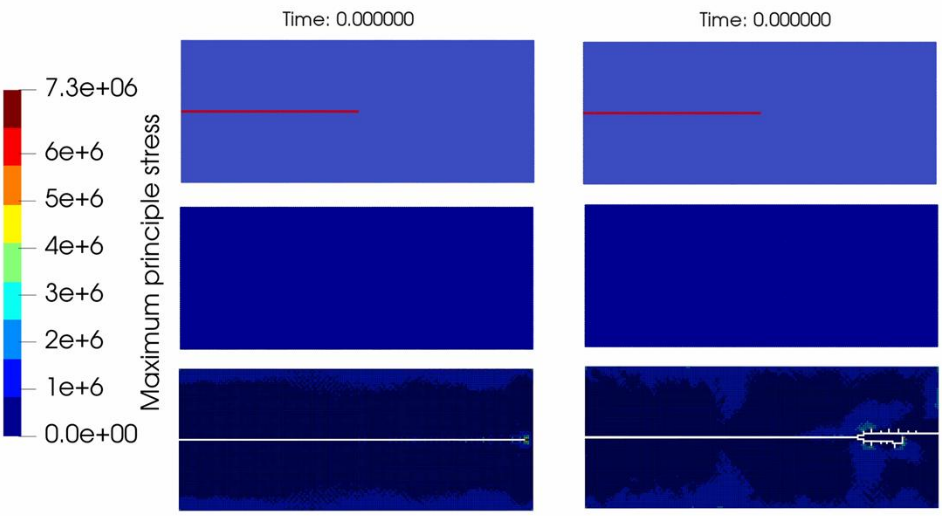

Dynamic Fracture

- **Problem description** Linear elasticity, $\rho_R = 2700$ kg m^{-3}, $E = 71.4$ GPa, Poisson's ratio $\nu = 0.25$, maximum principal stress $S_{\max} = 344.862$ MPa.

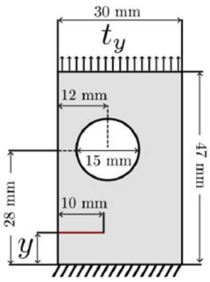

$$t_y = \begin{cases} 22 \text{ MPa} & \text{when } y = 5 \text{ mm} \\ 26 \text{ MPa} & \text{when } y = 10 \text{ mm} \\ 28 \text{ MPa} & \text{when } y = 15 \text{ mm} \end{cases}$$

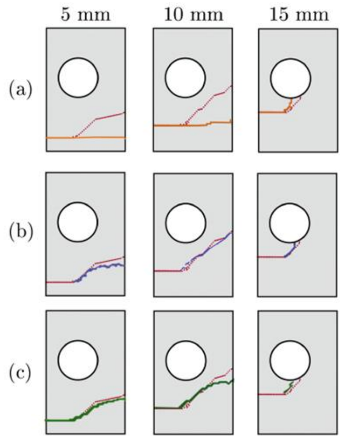

(a) Element deletion method [Song *et al.*, 2007]
(b) Pseudo-spring SPH [Islam *et al.*, 2020]
(c) Discrete element method [Kosteski *et al.*, 2012]

SUMMARY

- **Solid dynamics can be formulated as a set of 1st order conservation laws**
- **Using extended set of geometric variables allows for convex entropy extensions, in the form of the ballistic energy**
- **It is possible to extend the formulation to Arbitrary Lagrangian Eulerian in a robust manner**
- **In the context of Smooth Particle Hydrodynamics, the new formulation allows for stability and 2nd order convergence**
- **In linear elastodynamics the first order formulation allows for novel analytical solutions in dynamic crack propagation with intersonic and supersonic results**
- **The extension of these solutions to SPH permits a novel way to model dynamic crack propagation**

44

CIMNE

Publications:

- C. H. Lee, A. J. Gil, P. R. R. de Campos, J. Bonet, T. Jaugielavicius, S. Joshi and C. Wood. A Novel ALE SPH Algorithm for nonlinear solid dynamics, CMAME, 2024. [Open Access].
- Runcie, C.J., Lee, C.H., Haider, J., Gil, A.J., Bonet, J., An acoustic Riemann solver for large strain computational contact dynamics, (2022) IJNME, DOI: 10.1002/nme.7085
- Ghavamian, A., Lee, C.H., Gil, A.J., Bonet, J., Heuzé, T., Stainier, L., An entropy-stable Smooth Particle Hydrodynamics algorithm for large strain thermo-elasticity, (2021) CMAME, DOI: 10.1016/j.cma.2021.113736
- Bonet, J., Gil, A.J., Mathematical models of supersonic and intersonic crack propagation in linear elastodynamics, (2021) Int. J. of Fracture, DOI: 10.1007/s10704-021-00541-y
- Bonet, J., Lee, C.H., Gil, A.J., Ghavamian, A., A first order hyperbolic framework for large strain computational solid dynamics. Part III: Thermo-elasticity, (2021) CMAME, DOI: 10.1016/j.cma.2020.113505
- Hassan, O.I., Ghavamian, A., Lee, C.H., Gil, A.J., Bonet, J., Auricchio, F., An upwind vertex centred finite volume algorithm for nearly and truly incompressible explicit fast solid dynamic applications: Total and Updated Lagrangian formulations, (2019) JCP: X, DOI: 10.1016/j.jcpx.2019.100025
- Lee, C.H., Gil, A.J., Ghavamian, A., Bonet, J., A Total Lagrangian upwind Smooth Particle Hydrodynamics algorithm for large strain explicit solid dynamics, (2019) CMAME, DOI: 10.1016/j.cma.2018.09.033
- Haider, J., Lee, C.H., Gil, A.J., Bonet, J., A first-order hyperbolic framework for large strain computational solid dynamics: An upwind cell centred Total Lagrangian scheme, (2017) IJNME, DOI: 10.1002/nme.5293
- Lee, C.H., Gil, A.J., Greto, G., Kulasegaram, S., Bonet, J., A new Jameson–Schmidt–Turkel Smooth Particle Hydrodynamics algorithm for large strain explicit fast dynamics, (2016) CMAME, DOI: 10.1016/j.cma.2016.07.033
- Aguirre, M., Gil, A.J., Bonet, J., Lee, C.H., An upwind vertex centred Finite Volume solver for Lagrangian solid dynamics, (2015) Journal of Computational Physics, DOI: 10.1016/j.jcp.2015.07.029
- Bonet, J., Gil, A.J., Lee, C.H., Aguirre, M., Ortigosa, R., A first order hyperbolic framework for large strain computational solid dynamics. Part I: Total Lagrangian isothermal elasticity, (2015) CMAME, DOI: 10.1016/j.cma.2014.09.024
- Aguirre, M., Gil, A.J., Bonet, J., Arranz Carreño, A., A vertex centred Finite Volume Jameson-Schmidt-Turkel (JST) algorithm for a mixed conservation formulation in solid dynamics, (2014) JCO, DOI: 10.1016/j.jcp.2013.12.012

45

CIMNE

Acknowledgements

Proyecto PID2022-141957OB-C21 financiado por MICIU/AEI/10.13039/501100011033/ FEDER, UE

46